

A Scenario of Storm Surge Statistics for the German Bight at the Expected Time of Doubled Atmospheric Carbon Dioxide Concentration

HANS VON STORCH AND HINRICH REICHARDT

Institute of Hydrophysics, GKSS Research Centre, Geestthacht, Germany

(Manuscript received 5 June 1996, in final form 25 March 1997)

ABSTRACT

Past variations of water levels at Cuxhaven, Germany (German bight), are examined, and a scenario for future changes due to expected global warming is derived.

The observational record of Cuxhaven water levels features a linear upward trend in the annual mean water level of about 30 cm 100 yr⁻¹ overlaid by irregular variations due to synoptic disturbances. These irregular storm-related variations are shown to have remained mostly stationary since the beginning of observations until today.

A scenario for future conditions is derived by means of a two-step downscaling approach. First, a "time slice experiment" is used to obtain a regionally disaggregated scenario for the time mean circulation for the time of expected doubling of atmospheric CO₂ concentrations. Then, an empirical downscaling model is derived, which relates intramonthly percentiles of storm-related water-level variations at Cuxhaven to variations in the monthly mean air pressure field over Europe and the northern North Atlantic.

Past variations of storm-related intramonthly percentiles are well reproduced by the downscaling model so that the statistical model may be credited with skill. The combined time slice–statistical model "predicts," for the expect time of doubled atmospheric CO₂ concentrations in the decade around 2035, an insignificant rise of the 50%, 80%, and 90% percentiles of storm-related water-level variations in Cuxhaven of less than 10 cm, which is well within the range of natural interdecadal variability. These numbers have to be added to the rise in mean sea level due to thermal expansion and other slow processes.

1. Introduction

Now that climate models comprising detailed models of the ocean and the atmosphere and their complex interaction have matured, they have become tools routinely used to derive so-called scenarios of possible future climate change (e.g., Cubasch et al. 1992; Manabe et al. 1991). Such scenarios represent plausible development that might occur if humanity increases its emissions of radiatively active gases into the atmosphere, as expected by the Intergovernmental Panel of Climate Change (Houghton et al. 1992).

Such models produce global distributions of all kinds of relevant quantities, such as precipitation and surface wind. Unfortunately, the robustness of these numbers decreases with decreasing spatial and temporal scales; local details are hardly resolved by the finite-sized grids, and a coast is reduced to a mere discontinuity of some properties. Also, for most commonly used climate models, the synoptic variability is insufficiently represented so that the statistics of storms and their strong, and

sometimes harmful, winds are not resolved (von Storch 1995a).

However, there is serious concern among the general public, in industries such as offshore oil (von Storch et al. 1993a) and insurance, and in governmental and administrative institutions that the storm climate may worsen in the future. There is no robust evidence for an ongoing worsening of the extratropical storm climate in the northeast Atlantic (WASA 1995), but general circulation models (GCMs) point to a moderate intensification of the frequency or strength of storms at the time of double carbon dioxide concentrations in the atmosphere (von Storch et al. 1993a; Lunkeit et al. 1996; Beersma et al. 1997).

Of particular concern is the future evolution of storm surge statistics at storm-ridden coasts, such as the North Sea coast, since such surges represent a significant threat to people's welfare. In the present paper, we deal with the evolution of water levels in the German bight, or more specifically, at the tide gauge of Cuxhaven, Germany (approximately 53°N, 9°E). We design a two-step downscaling approach to derive future storm surge scenarios for the anticipated time of double CO₂ concentrations in the atmosphere.

We emphasize the interpretation of a scenario as a "plausible evolution consistent with our *present* knowl-

Corresponding author address: Prof. Hans von Storch, Institut für Gewässerphysik, GKSS Research Centre, Max-Planck Straße, D-21502 Geestthacht, Germany.
E-mail: storch@gkss.de

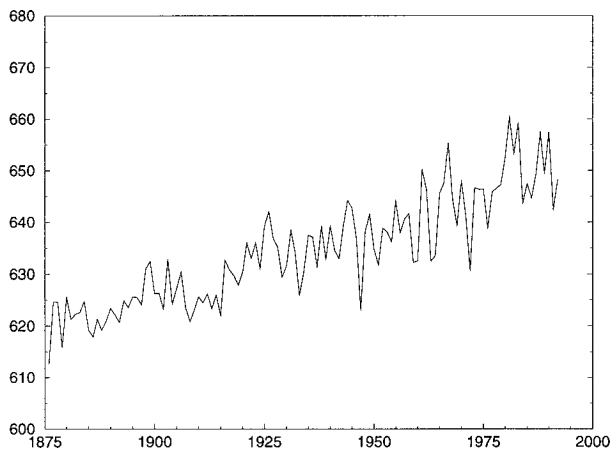


FIG. 1. Annual high-tide water level in Cuxhaven from the beginning of recording in 1876 to 1993. Units are centimeters.

edge.” In our case, in particular, the scenario depends crucially on the validity of the driving GCM experiment hierarchy (for details, see below). Thus, the scenario presented in this paper is our best guess *at this time* and may be replaced by other estimates when more robust GCM estimates have become available. However, we are confident that our method for building a consistent scenario will remain a valid tool.

The paper is organized as follows. After an overview of the data we have used (section 2), we outline our downscaling strategy in section 3. The statistical element in the downscaling strategy is a regression model based on canonical correlation analysis (CCA; section 4); the skill of this model is determined by applying it to independent data in section 5. The scenario for the time of expected doubled atmospheric CO_2 concentrations is given in section 6, and the paper is concluded in section 7 with a summary and some remarks.

2. Data

In the following we make use of two observational datasets and one GCM-simulated dataset.

One observational dataset features the water levels of high tides at Cuxhaven from 1876 to 1993. With a lunar tide of about 12 h and 25 min, approximately two observations per day are available. This time series reflects various processes, ranging from the effect of storm-related winds, the annual cycle, and sinking of the land to changes of the tidal dynamics caused by human modifications of the coastline and the Elbe River's bottom topography. The mean sea level in Cuxhaven has undergone a significant upward trend (Fig. 1) so that the mean level of the high tide in 1990 was about 30 cm above the level at the beginning of the recording in 1876.

We obtain the variations of storm-related water level by subtracting the long-term trend of annual mean water levels depicted in Fig. 1. By this operation, possible

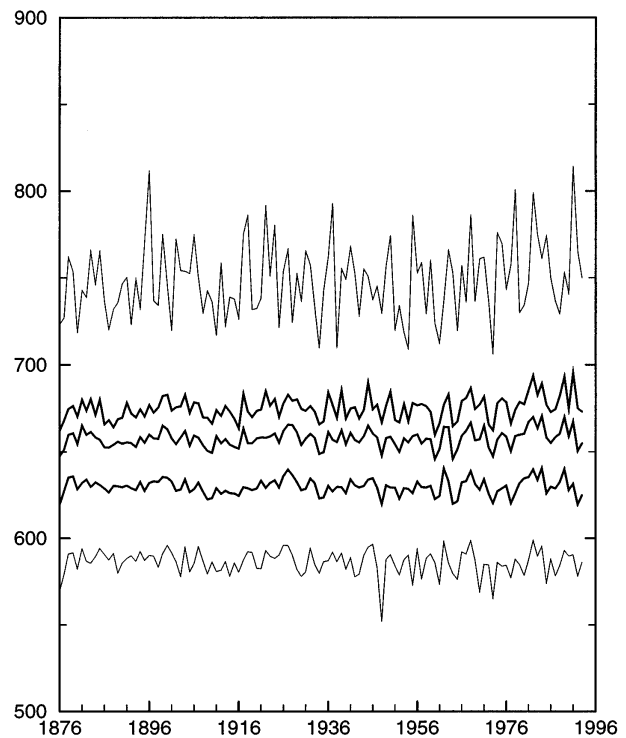


FIG. 2. Annual percentiles of the approximately twice-daily high-tide water levels at Cuxhaven after subtraction of the linear trend in the annual mean. From top to bottom, 99%, 90%, 80%, 50%, and 10% percentiles. The 90%, 80%, and 50% percentiles used in the sequel are drawn in bold. Units are centimeters.

creeping inhomogeneities are averted, which may arise from a variety of processes, such as trends reflecting eustatic or isostatic sea level rise, or slow adjustments to anthropogenic interferences like dredging of harbors.

Figure 2 illustrates the absence of trends in the percentiles of these storm-related water level variations. In the last few years, the percentiles have been somewhat larger than previously, but these increased values do not represent a systematic tendency and may very well be a reflection of natural variability in the climate system. Thus, the ongoing trend toward higher storm surges is mostly due to an increase in the mean high tides and *not in a change of storminess*. This finding is consistent with Schmidt and von Storch (1993), who found no indications of a systematic worsening of the storm climate in a long time series of geostrophic winds in the German bight (see also WASA 1995, Kaas et al. 1996).

The other observational dataset comprises monthly analyses of the distribution of air pressure over western Europe and the northern North Atlantic (30° – 70° N, 70° W– 25° E) from 1899 to 1988. These analyses have been prepared by different weather services. The daily analyses have continuously been improved so that the daily analyses are inhomogeneous, containing a spurious signal of a roughening storm climate. The monthly analyses, however, are believed to be mostly homoge-

neous and unaffected by significant inhomogeneities (Trenberth and Paolino 1980).

Monthly mean air pressure maps for the western European–northern North Atlantic area are also available from a time slice GCM experiment (see below in section 3a). This GCM experiment was executed for 6 model years. All maps are given anomalies—that is, as deviations from a 5-yr mean of a control representing present day conditions (cf. Cubasch et al. 1995).

3. The downscaling strategy to derive scenarios

The idea of “downscaling” is to build a dynamic or statistical model that relates large-scale features to local features of interest. If the large-scale features are well simulated by a climate model, then the link may be used to postprocess the GCM output and scenarios of local climate change may be determined (Hewitson and Crane 1992; von Storch et al. 1993b). The paradigm behind this approach is that the large-scale climate of the atmosphere is determined by planetary-scale features, such as the distributions of continents and mountains and the latitudinal variation of incoming radiation. Then, the local climate appears as the result of an interplay of the large-scale climate and the local details, such as the details of a coast, of land use and of smaller orographic features.

In the present paper, a twofold downscaling strategy is pursued. First, a dynamic downscaling is made with the help of a “time slice” experiment (see section 3a). In this way, an estimate of the expected changes of the monthly mean air pressure distribution in the area of western Europe and the northeast Atlantic is derived. In the second step, this monthly mean air pressure distribution is related to intramonthly percentiles of tide levels in Cuxhaven (German bight) through a statistical regression model.

a. Time slice experiment

A time slice experiment with an atmospheric model is a means of describing climate change with high resolution, which can not be done in the straightforward manner of integrating a fully coupled atmosphere–ocean model because of the enormous computational costs of such an exercise. With present-day technology, simulations of the atmospheric dynamics with a horizontal resolution of T106 (corresponding to about 70 km) can be integrated for 5–10 yr. Such an integration is very costly, and an integration over 100 or more years is simply impossible at this time. If the demand for horizontal resolution is relaxed and a moderate resolution, such as T42 (approximately 300-km horizontal grid spacing) is used, tens of years can be integrated.

The time slice experiment approach (Cubasch et al. 1995) for inferring high-resolution information accepts the large-scale features in sea surface temperature (SST) and sea ice distribution simulated in coarse resolution

for example, T21 (corresponding to about 600-km grid sizes), atmosphere–ocean models as sufficiently good estimates of expected climate change. Using this boundary conditions, a high-resolution atmospheric model is used for simulating the equilibrium response to the changed SST, sea ice coverage, and, possibly, carbon dioxide concentrations. Such experiments are named time slice experiments, a term originating from simulations of paleoclimatic conditions, in which estimates of paleoclimatic SST, sea ice coverage, and land–sea distribution were processed.

In the present case, we make use of a pair of T106 time slice experiments done by Bengtsson et al. (1995, 1996), which were designed for building a high-resolution scenario for the expected time of doubling carbon dioxide concentrations in the atmosphere—that is, for the decade around 2050. In their base run (Bengtsson et al. 1995), they used present day carbon dioxide concentrations and present day SST and sea ice coverage. In their “ $2 \times \text{CO}_2$ ” simulation (Bengtsson et al. 1996), they prescribed atmospheric doubled carbon dioxide concentrations and modified the SST and sea ice distribution by adding anomalies simulated in a coarse resolution atmosphere–ocean simulation of the “business as usual” scenario of global warming (an increase of the CO_2 concentration of about $1\% \text{ yr}^{-1}$; Cubasch et al. 1992). These anomalies are the differences between the SST and sea ice coverage simulated by the coarse resolution model in the decade around the model year 1985 and around the model year 2050. The resulting SST anomaly, which is superimposed on present SST in the $2 \times \text{CO}_2$ -time slice experiment, is shown in Fig. 3. When forced with such an anomalous SST and exposed to doubled CO_2 concentrations, the T106 atmospheric GCM responds with the mean air pressure distribution displayed in Fig. 4.

This time slice experiment has been examined with respect to several aspects of regional climate, such as the Indian monsoon (Lal et al. 1995), southern Europe (Cubasch et al. 1996), and other regions (Cubasch et al. 1995). Statistics of tropical storms have been studied by Bengtsson et al. (1995, 1996) and statistics of North Atlantic storms by Beersma et al. (1997). According to Beersma et al. (1997), the five-winter mean air pressure distribution in the T106 control run is consistent with the 1990–95 observations but deviates from the 1985–89 observations, indicating the impact of interdecadal variability on time means of only five winters.

Additionally, a pair of 30-yr time slice experiments with the same experimental setup and atmospheric model, but with a reduced horizontal resolution of T42, is available (Cubasch et al. 1995, 1996).

An alternative for using the time slice experiment would be to use anomalous air pressure distributions simulated in the coarse resolution model; since this model suffers from some systematic errors in the North Atlantic area (Cubasch et al. 1992), we prefer not to do so.

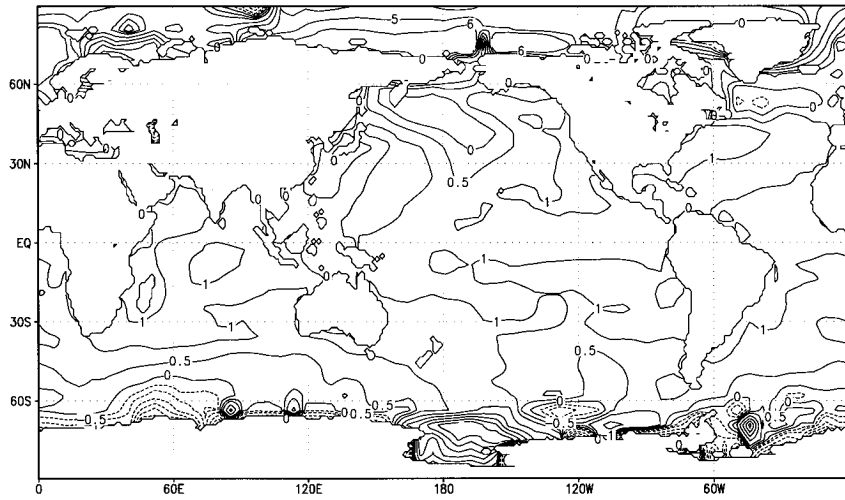


FIG. 3. Sea surface temperature obtained in the base climate change run for the time slice 2035. This anomalous distribution is superimposed on the present SST distribution in the T106 time slice experiment.

b. The empirical model

The second step of the downscaling model consists of an empirical model, which relates the monthly mean air pressure distribution over a large area covering western Europe and the northeast Atlantic to intramonthly percentiles of storm-related water-level variations at Cuxhaven. The κ percentile $q_{\kappa,t}$ in a month t is defined to be that water level for which a κ fraction of detrended water levels $w_{t,k}$ in the considered month t is smaller than $q_{\kappa,t}$:

$$\frac{\#\{w_{t,j} < q_{\kappa,t}; j = 1 \dots T_t\}}{T_t} \leq \kappa, \quad (1)$$

where the symbol “ $\#\{\dots\}$ ” represents the number of elements in a set and T_t is the number of observations in the month t . Thus, in a month with 60 observations, the 90% percentile is the sixth largest observation in that month. Fifty-three observations are smaller than the percentile and 5 are larger.

The empirical model is based on a canonical corre-

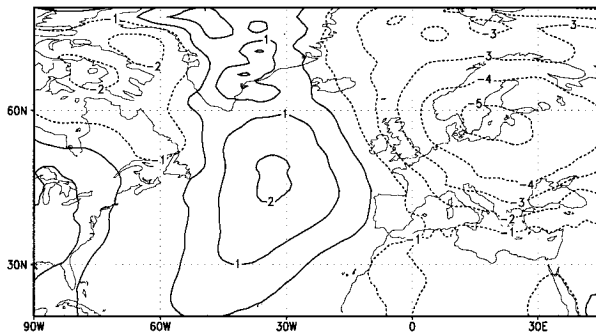


FIG. 4. Anomalous winter (DJF) mean air pressure anomaly simulated in the time slice experiment as a response to modified SST and doubled CO_2 concentrations.

lation analysis, which links two sets of random vectors (Barnett and Preisendorfer 1987; von Storch 1995b). In the present analysis, one vector time series \mathbf{S} , is formed by the coefficients of the first four empirical orthogonal functions (EOFs) of winter [December–February (DJF)] monthly mean air pressure distributions. Prior to the EOF analysis, the air pressure data were centered; that is, the long-term mean distribution was subtracted so that anomalies were obtained. The other vector time series \mathbf{Q} , is three-dimensional, featuring the 50%, 80%, and 90% percentiles of winter intramonthly storm-related water-level distributions:

$$\mathbf{Q}_t = \begin{pmatrix} q_{50\%} \\ q_{80\%} \\ q_{90\%} \end{pmatrix}_t. \quad (2)$$

The result of a CCA is pairs of vectors ($\mathbf{p}^{s;k}$, $\mathbf{p}^{q;k}$) and time coefficients $\alpha_{s;k}(t)$ and $\alpha_{q;k}(t)$ so that

$$\mathbf{S}_t = \sum_k \alpha_{s;k}(t) \mathbf{p}^{s;k}$$

and

$$\mathbf{Q}_t = \sum_k \alpha_{q;k}(t) \mathbf{p}^{q;k}. \quad (3)$$

The time coefficients are uncorrelated for different indices k :

$$\text{Cov}(\alpha_{s;k}, \alpha_{s;j}) = \text{Cov}(\alpha_{q;k}, \alpha_{q;j}) = 0$$

and

$$\text{Cov}(\alpha_{s;k}, \alpha_{q;j}) = 0. \quad (4)$$

The $k = 1$ coefficients share a maximum correlation, the $k = 2$ coefficients another maximum correlation obtainable under the constraint (4), and so forth. In the present setup, with only three components in the \mathbf{Q} vec-

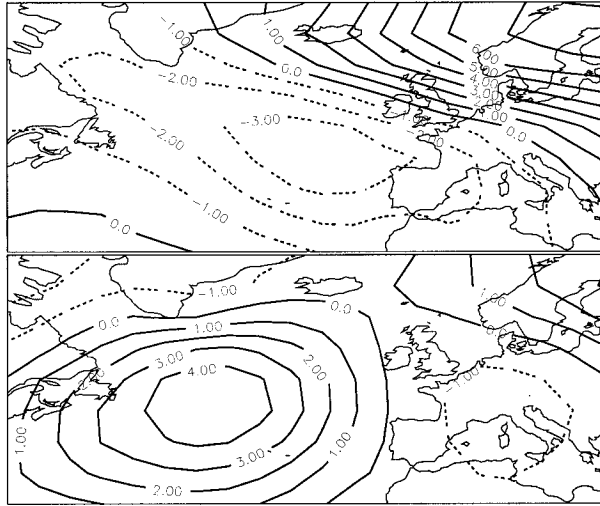


FIG. 5. First two characteristics patterns $\mathbf{p}^{s:1}$ (top) and $\mathbf{p}^{s:2}$ (bottom) of monthly mean air pressure anomalies over the northeast Atlantic. The coefficients of these CCA vectors share a maximum correlation with the coefficients of the water-level percentile patterns given in Table 1. Units are hPa.

tor, a maximum of three nonzero correlations may be obtained.

The CCA is usually applied to “anomalies”—that is, to data whose long-term mean has been subtracted. In the present case, the air pressure data were already centered before the EOF analysis; the percentiles of the water level are calculated from the detrended data. The \mathbf{Q} vector is then formed by the anomalies of each of the three percentiles.

The vectors ($\mathbf{p}^{s:k}$, $\mathbf{p}^{q:k}$) are interpreted as characteristic patterns. In the present analysis, the coefficients are normalized to one:

$$\text{Var}(\alpha_{q;k}) = \text{Var}(\alpha_{s;k}) = 1$$

so that the three components of $\mathbf{p}^{q:k}$ may be interpreted as anomalies that typically occur together with the “field distribution” $\mathbf{p}^{s:k}$.

The downscaling model, which relates the large-scale air pressure information to the local-scale storm-related water-level information, is a regression model for the CCA coefficients $\alpha_{s;k}$ and $\alpha_{q;k}$, with a reconstruction in the three-dimensional space using (3):

$$\hat{\alpha}_{q;k}(t) = \rho_k \alpha_{s;k}(t) \quad (5)$$

and

$$\mathbf{Q}_t = \begin{pmatrix} q_{50\%} \\ q_{80\%} \\ q_{90\%} \end{pmatrix}_t = \sum_{k=1}^K \hat{\alpha}_{q;k}(t) \mathbf{p}^{q:k}. \quad (6)$$

The coefficient $\alpha_{s;k}$ at time t could be obtained by forming the dot product of the air pressure field \mathbf{S}_t and the adjoint CCA pattern $\mathbf{p}^{s:k}$. However, the adjoints have to fulfill orthogonality conditions with all other CCA patterns so that they tend to be sensitive to the truncation

TABLE 1. Characteristic anomalies of intramonthly percentiles of storm-related water-level variations in winter (DJF) at Cuxhaven. The k row is the k th CCA vector $\mathbf{p}^{q:k}$. This vector represents ϵ_k of the variance of \mathbf{Q} within the fitting interval December 1970–February 1988. Its coefficient $\alpha_{q;k}$ shares a correlation of ρ_k with the coefficient of the air pressure pattern $\mathbf{p}^{s:k}$ within the fitting interval.

$\kappa =$	50%	80%	90%	ϵ_k	ρ_k
k		(cm)		(%)	
1	−21	−16	−18	83	0.89
2	−10	1	10	13	0.32
3	−2	7	−3	4	0.16

of the a priori EOF projection. Therefore, we determine the CCA coefficients $\alpha_{s;k}$ as a least squares fit by minimizing

$$\left\| \mathbf{S}_t - \sum_{k=1}^K \alpha_{s;k} \mathbf{p}^{s:k} \right\|. \quad (7)$$

The regression model of (5) and (6) may be applied to anomalies of observed or simulated air pressure fields.

In section 4, we show and discuss the resulting patterns $\mathbf{p}^{q:k}$ and $\mathbf{p}^{s:k}$ and their relationship. The skill of the regression model of (5) and (6) in reproducing past storm-related water-level variations is presented in section 5. Finally, in section 6, the regression model of (5) and (6) is used to postprocess the monthly mean air pressure distributions from the $2 \times \text{CO}_2$ time slice climate change experiment.

4. The CCA patterns

The CCA is done with the 19-yr subset of data from December 1970 to February 1988. The remaining data, prior to 1970, are kept as independent data to verify the statistical model.

As already mentioned, a maximum of three pairs of patterns with nonzero correlations may be obtained. These correlations, derived from the fitting interval 1970–88, amount to 0.89, 0.32, and 0.16. We will see in section 5 that the positive correlation of the third pair reflects merely sample variations and does not contribute to the skill of the model of (5) and (6). Therefore, we limit ourselves in the remainder to the first two CCA pairs.

The air pressure distributions, which are connected with characteristic storm-related water levels, are shown in Fig. 5. The associated anomalies of storm-related intramonthly water-level percentiles are given in Table 1.

The first air pressure anomaly pattern $\mathbf{p}^{s:1}$ describes a southeasterly flow across the North Sea, which is connected with an almost uniform decrease of all three considered percentiles (first row in Table 1) of -20 cm. If the amplitude of the air pressure pattern is doubled, then the percentiles are lowered by about -40 cm; when the sign of the amplitude is reversed, the percentiles are increased by about 20 cm. This CCA pair describes the dominant atmospheric control of water-level varia-

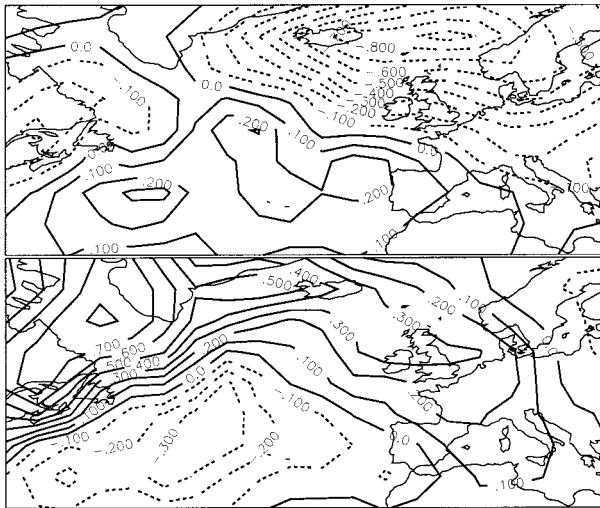


FIG. 6. Regression patterns of the standard deviation of intramonthly high-pass-filtered variance of daily air pressure fields to the CCA coefficients $\alpha_{s;k}$. (Top) $k = 1$. (Bottom) $k = 2$.

tions—as much as 83% of the (sample) variance of month-to-month variability of intramonthly percentiles is represented by this first pair of patterns.

The monthly mean anomaly of air pressure is connected with a characteristic pattern of storminess. For that purpose, we identify the storminess by the intramonthly standard deviation calculated from high-pass-filtered air pressure variations σ_{SLP} . The high pass-filter maintains the “synoptic timescale” variability between 2.5 and 6 days. The link between the monthly mean anomaly and this measure of storminess is established by computing regression maps between the CCA coefficients $\alpha_{s;k}(t)$ and the vector time series σ_{SLP} at all locations. The CCA patterns $\mathbf{p}^{s;k}$ shown in Fig. 5 are linearly connected with the regression maps in Fig. 6: If the monthly mean map is as in Fig. 5, then on average the anomalous storminess will be as in Fig. 6; if the monthly mean anomaly is doubled (sign reversed), then the expected distribution of anomalous storminess is doubled (sign reversed).

From the distributions shown in Fig. 5 and 6, we conclude that the first CCA pattern encompasses two related factors affecting water-level variations. First, there is a weakened mean northwesterly flow; second, this pattern reduces the formation of synoptic disturbances that travel in a southeasterly direction into the North Sea, where they pile up water in the German bight.

Two time series of high-tide levels with a large positive and a large negative CCA coefficient $\alpha_{q;1}$ are displayed in Fig. 7. The January 1983 time series is characterized by a general increase of water levels—not only of the extremes, but also of the time average; its CCA coefficient amounts to $\alpha_{q;1} = -2.4$, indicating an overall shift of the distribution by about $2.4 \times 20 \text{ cm} \approx 50 \text{ cm}$ relative to the time mean conditions. Indeed, the anom-

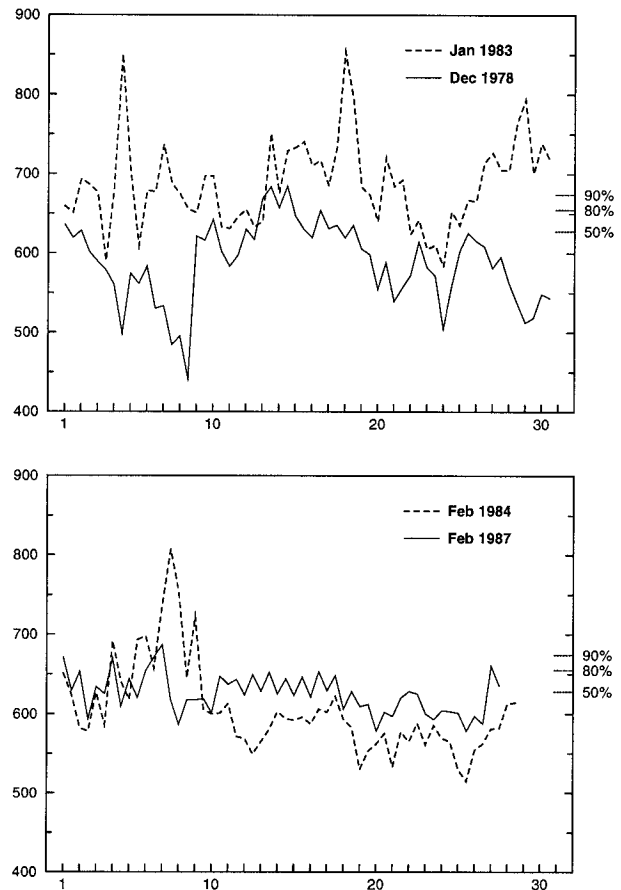


FIG. 7. Time series of high-tide levels monitored at Cuxhaven during selected months with large positive, or negative, CCA coefficients $\alpha_{q;k}$. Vertical axes: water levels in centimeters. Horizontal axes: time in days. The climatological mean values of the 50%, 80%, and 90% percentiles are given as tick marks on the left margin of the diagrams. (Top) $k = 1$, displaying January 1983 and December 1978. (Bottom) $k = 2$, with Februaries 1987 and 1993.

alies of the 50%, 80%, and 90% percentiles are 58, 62, and 50 cm. The opposite effect took place in December 1978, when water levels were generally lower, with 50%, 80%, and 90% percentile anomalies of -24 , -39 , and -47 cm . The CCA coefficient in that month is $\alpha_{q;1} = 1.8$ so that the expected overall decrease is $1.8(-20) \text{ cm} \approx -35 \text{ cm}$. Obviously, the first CCA pair is powerful in representing interannual variability in the percentiles.

The second air pressure pattern $\mathbf{p}^{s;2}$ is considerably less important for the variations of Cuxhaven water levels since it represents in the fitting interval no more than 13% of the variance of the combined vector of percentile anomalies. Its link to water-level variations is rather different from that of the first CCA pattern: the 50% percentile is lowered by 10 cm, the 80% percentile is almost unchanged, and the 90% percentile is lifted by 10 cm. Thus, the water-level distribution becomes markedly broader if this air pressure distribution prevails; if the sign of air pressure anomaly is reversed, then the

TABLE 2a. The skill of the regression model of (5) and (6) for different numbers K , determined from independent data (1899–1969), as given by the correlation ρ_κ of the intramonthly percentile p as derived from in situ observations and from the regression model (5) and (6).

K	$\kappa =$	Correlation skill score ρ_κ		
		50%	80%	90%
1		0.75	0.73	0.69
2		0.79	0.72	0.63
3		0.79	0.72	0.63

TABLE 2b. As in Table 2a but for percentage ϵ_κ of the month-to-month variability of the intramonthly percentile q_κ represented by the regression model (5) and (6).

K	$\kappa =$	Represented variance ϵ_κ		
		50%	80%	90%
1		53%	50%	45%
2		62%	50%	40%
3		62%	49%	40%

water-level distribution tends to be narrower than normal.

Also, the second pair of CCA pairs is physically plausible. The anomalous air pressure distribution of $\mathbf{p}^{s,2}$ in Fig. 5 does not cause an additional accumulation of water in the German bight. Indeed the mean air flow across the North Sea is southeasterly, and, consistently, the 50% percentile is reduced. However, this pattern steers occasionally energetic synoptic disturbances into the area of the North Sea (Fig. 6, bottom) so that the higher percentiles are enhanced.

In Fig. 7, time series of high-tide levels for 2 months are shown, which have little contribution from the first CCA pair and relatively large $\kappa = 2$ coefficients: in February 1984, they are $\alpha_{q,1} = 0.82$ and $\alpha_{q,2} = 2.6$. The 50% percentile in that month is 34 cm smaller than in the long-term mean, but the 90% percentile is, due to one storm event in the first third of the month, increased by 23 cm. An opposite case is represented by February 1987, when $\alpha_{q,2} = -1.3$ is negative and $\alpha_{q,1} = 0.01$ is negligible. The 50% percentile is slightly increased, by 7 cm, but the high tides do not really vary in February 1987, so the 90% percentile is reduced by 21 cm.

5. The skill of the regression model (5) and (6)

The CCA analysis explores properties of the sample of monthly data from 20 consecutive winters. However, the CCA is known to overestimate the correlation among the patterns (Glynn and Muirhead 1978), so it is mandatory to check the quality of the resulting regression model with independent data.

Therefore, the regression model (5) and (6) has been used to estimate intramonthly percentiles for Cuxhaven for the winters 1899 to 1988. (Unfortunately, no air pressure maps are available for the years before 1899, while water levels have been recorded in Cuxhaven since 1876.) The success of the reconstruction of observed intramonthly water-level percentiles is quantified by two measures of skill, namely the correlation skill score ρ_κ and the percentage of represented variance ϵ_κ for $\kappa = 50\%$, 80% , and 90% :

$$\rho_\kappa = \frac{\text{Cov}(\hat{q}_{\kappa,t}, q_{\kappa,t})}{\sqrt{\text{Var}(\hat{q}_{\kappa,t})\text{Var}(q_{\kappa,t})}}$$

and

$$\epsilon_\kappa = 1 - \frac{\text{Var}(\hat{q}_{\kappa,t} - q_{\kappa,t})}{\text{Var}(q_{\kappa,t})}, \tag{8}$$

where $\hat{q}_{\kappa,t}$ is the estimated κ percentile in the month t . For the general concept of skill scores, the reader is referred to Livezey (1995).

The skill of our downscaling model has been determined by calculating (5) and (6) with the data from 1899 to 1969, which have not been used for fitting the model (Table 2). The best results, both in terms of local correlations and in variance accounted for, are obtained when the first ($K = 1$) or the first two CCA pairs ($K = 2$) are used; the addition of the third pair of patterns does not further increase the skill.

The inclusion of the second canonical pair improves the skill for the 50% percentile but reduces the skill for the 90% percentile. We include it in the regression model in order to have more degrees of freedom for the evaluation of the time slice scenario.

As in most cases with statistical models, a marked percentage of variance is *not* represented by the model. This “failure” matters if the goal of the model is to reproduce the details of a development. In the present case, however, these details do not matter; instead, all that is needed are the statistics of storm-related water-level variations. The achievement of this goal is demonstrated by Fig. 8, which displays the time series of the percentiles as derived from the detrended in situ observations and as reconstructed by the regression model (5) and (6). The differences between the in situ data and the indirectly derived data appear to be of mostly a short-term character. A spectral analysis reveals that the regression model underestimates the variance mostly for the high-frequency variations (not shown).

6. The scenario

In order to determine a consistent scenario of expected future storm-related water levels in Cuxhaven, the mean difference field of air pressure in the “ $2 \times \text{CO}_2$ ” and the “control” T106 time slice experiment (see Fig. 4) is plugged into the regression model (5) and (6). (The difference field is well represented by the first four EOFs of the observed sea level pressure variability: only 20% of the variance are discarded.)

The time mean CCA coefficients simulated in the GCM experiments are $\alpha_{s,1} = -0.40$ and $\alpha_{s,2} = 0.26$. Thus, the distribution of storm-related water-level

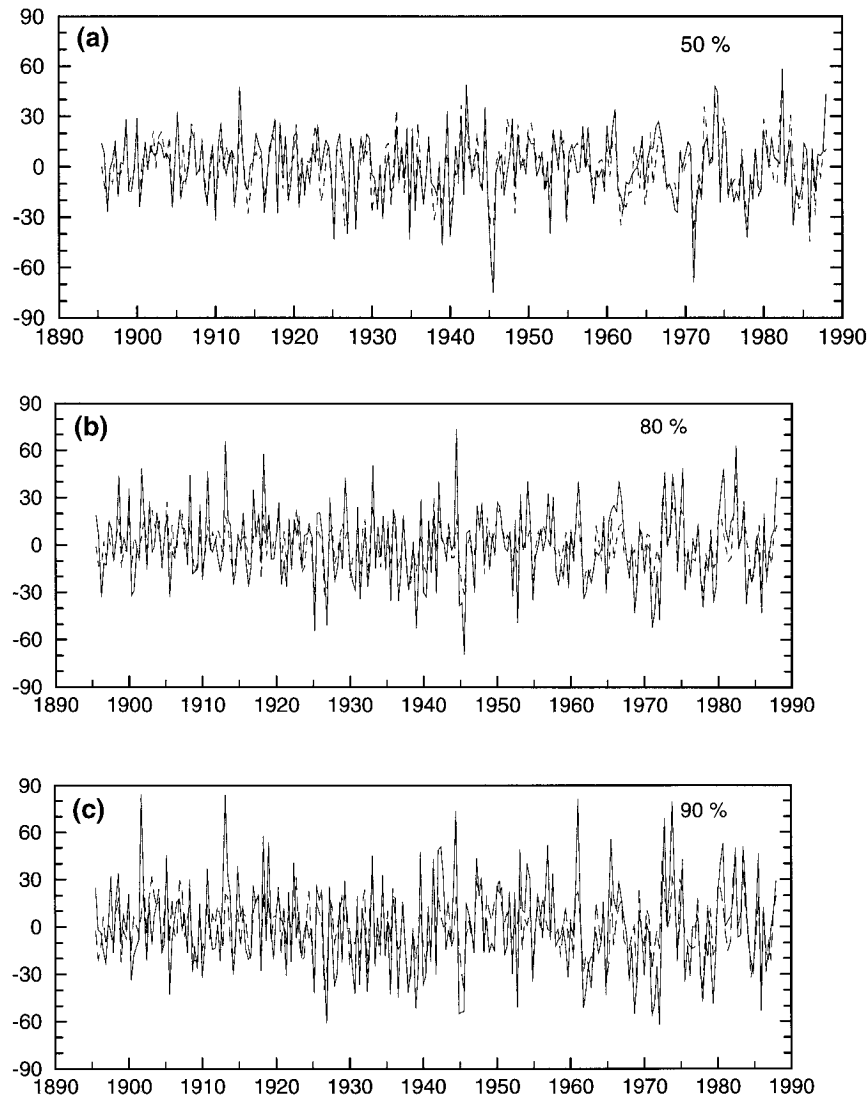


FIG. 8. Time series of p percentiles of intramonthly storm-related water-level variations in Cuxhaven, as derived from in situ observations (solid) and estimated from the monthly mean air pressure field through (5) and (6) (dashed). Units are centimeters: (a) $p = 50\%$, (b) $p = 80\%$, and (c) $p = 90\%$.

variations is shifted slightly toward larger values; the expected changes are 7, 6, and 7 cm for the 50%, 80%, and 90% percentiles, respectively.

At this time, a word of caution is required. The above scenarios for changes of storm-related water levels at Cuxhaven are consistent with, and within the range of, previously observed water-level variations at Cuxhaven. As such, they are plausible. However, they depend crucially on the validity of the driving GCM experiments; if these GCM simulations prove to be inadequate, then also our numbers will be inadequate.

The scenario given above is mostly determined by the first CCA pair since the second CCA pair does not contribute significantly to the final numbers: the small

value of $\alpha_{s,2}$ is multiplied by the rather small value of $\rho_2 = 0.32$ [cf. (5)].

An alternative to the regression model (5) would be to use $\rho_\kappa = 1$ in (5). This alternative is motivated by the interpretation that $p^{q:1}$ tends to occur simultaneously with $p^{s:1}$. With this revised model, a slightly different scenario is derived, namely 6 cm for the 50% and the 80% percentile, and 9 cm for the 90% percentile.

The same procedure applied to a pair of 30-yr T42 time slice experiments gave consistent results (no diagrams shown). The first four EOFs describe 82% of the signal's variance. The derived increase of percentiles amounts to 8 cm for the median, 10 cm for the 80% quantile, and 11 cm for the 90% quantile.

7. Conclusions

The results of the present study may be summarized as follows.

- A canonical correlation analysis of monthly northeast Atlantic air pressure fields and vectors of several percentiles of intramonthly storm-related water levels in Cuxhaven returns two physically plausible connections.
- From the results of the CCA, a regression model can be built that specifies anomalies of water-level percentiles as a linear function of anomalous air pressure distributions.
- The regression model is capable of reproducing past variations of storm-related water levels in Cuxhaven. In the past, no significant increase of storm-related water levels has occurred.
- A scenario of possible future storm surge statistics is derived from a regular low-resolution climate run, by first executing high-resolution time slice experiments and then by applying the regression model to the high-resolution time mean air pressure fields.

An interesting by-product of the analysis is the finding that the statistical link between the sea level variations and the air pressure variations remains stationary throughout the whole dataset. This fact underlines the reliability of the air pressure analyses, which seem to be homogeneous through the course of time.

When presenting results from downscaling exercises, two types of questions are typically asked—namely, whether the adopted strategy is optimal and whether the numerical results are statistically “significant.” Both questions are not well taken, as is explained in the remaining paragraphs.

There are alternatives to our two-step downscaling strategy—whether these alternatives are more powerful in representing variance cannot be said a priori but must be tried. One alternative is to use the weather stream simulated in the time slice experiments to force a regular storm surge model. Indeed, such a study is presently under way, but results are not yet available. Another approach would make use of the “statistical–dynamical” downscaling approach of Frey-Buness et al. (1995). In that case, storms would be classified according to their ability to cause storm surges and the changing frequencies of these storm classes would be derived from the time slice experiment. Then, the frequencies would be transformed into water-level statistics by selecting for each class one or more “typical storms” and by forcing a storm surge model with these typical storms (see also Bijl et al. 1997).

The month-to-month standard deviations, derived from 18 monthly difference maps, of the downscaled percentiles are about 10 to 13 cm. Thus, the estimated changes of storm-related water levels are comparable to natural variations. Indeed, such values may merely re-

fect the interdecadal variability unrelated to global warming.

We suggest the use of our scenario of future water level as, for the time being, a good estimator of possible future developments. With all of the uncertainties involved, such as the timing of doubling CO₂, the treatment of a number of key processes in climate models, and the like, we honestly cannot offer *in any objective sense* error margins. However, we *believe* that these numbers are reasonable; they will certainly have to be revised after the availability of high-resolution time slice experiments with other GCMs. Indeed, one may rightly argue that a simulation of only 5 yr is too short for a proper discrimination between an externally forced (greenhouse) signal and the interdecadal variability (Beersma et al. 1997), but a longer simulation with such a high resolution is simply not available at this time.

Finally, an important limitation of the present study should be emphasized—we have dealt exclusively with changes of storm-related water levels. As pointed out by Cui et al. (1995), the sea level varies on timescales longer than the synoptic timescale of several days for various reasons. In case of global warming, the thermal expansion of the sea water (cf. Mikolajewicz et al. 1990; de Wolde et al. 1995), and the net growth or loss of land and shelf ice, as well as changing regional circulation patterns in the ocean, are of particular relevance for the slowly changing sea level. The changes of storm-related water-level variations must be understood as relative to such slowly changing “mean” levels (cf. Figs. 1 and 2).

Acknowledgments. We thank Lennart Bengtsson for his kind permission to use the T106 time slice experiments, which were executed as a collaborative project of the Eidgenössische Technische Hochschule in Zürich, Switzerland, and the Max-Planck-Institut für Meteorologie in Hamburg, Germany, at the Swiss Climate Computing Centre. We are grateful to Dr. Ulrich Cubasch for making the T42 time slice data available. We thank Drs. Annutsch and Huber who alerted us to the fact that the apparent rise of extreme water-level heights was due to a rise of the mean water level and supplied us with the data for Cuxhaven. Hauke Heyen and Dr. Eduardo Zorita have contributed significantly to this study by their ongoing support in technical matters and their presence as scientific sparring partners. Peter Wright gave valuable advice for the improvement of the English. Two anonymous reviewers helped with critical questions and constructive suggestions to greatly improve the clarity of the outlandish English. The present project was funded by the Bundesministerium für Bildung, Wissenschaft, Forschung und Technologie Project 03F0141B.

REFERENCES

- Barnett, T. P., and R. Preisendorfer, 1987: Origins and levels of monthly and seasonal forecast skill for United States surface air tem-

- perature determined by canonical correlation analysis. *Mon. Wea. Rev.*, **115**, 1825–1850.
- Beersma, J., K. Rider, G. Komen, E. Kaas, and V. Kharin, 1997: An analysis of extratropical storms in the North Atlantic region as simulated in a control and a $2 \times \text{CO}_2$ time-slice experiment with a high resolution atmospheric model. *Tellus*, **49A**, 347–361.
- Bengtsson, L., M. Botzet, and M. Esch, 1995: Hurricane-type vortices in a general circulation model. *Tellus*, **47A**, 175–196.
- , —, and —, 1996: Will greenhouse gas-induced warming over the next 50 years lead to higher frequency and greater intensity of hurricanes? *Tellus*, **48A**, 57–73.
- Bijl, W., 1997: Impact of a wind climate change on the surge in the southern North Sea. *Climate Res.*, **8**, 45–49.
- Cubasch, U., K. Hasselmann, H. Höck, E. Maier-Reimer, U. Mikolajewicz, B. D. Santer, and R. Sausen, 1992: Time-dependent greenhouse warming computations with a coupled ocean–atmosphere model. *Climate Dyn.*, **8**, 55–69.
- , J. Waskewitz, G. C. Hegerl, and J. Perlwitz, 1995: Regional climate changes as simulated in time-slice experiments. *Climate Change*, **31**, 273–304.
- , H. von Storch, J. Waskewitz, and E. Zorita, 1996: Estimates of climate change in southern Europe using different downscaling techniques. *Climate Res.*, **7**, 129–149.
- Cui, M., H. von Storch, and E. Zorita, 1995: Coastal sea level and the large-scale climate state: A downscaling exercise for the Japanese Islands. *Tellus*, **47A**, 132–144.
- de Wolde, J., R. Bintanja, and J. Oerlemans, 1995: On thermal expansion over the last hundred years. *J. Climate*, **8**, 2881–2891.
- Frey-Buness, F., D. Heimann, and R. Sausen, 1995: A statistical-dynamical downscaling procedure for global climate simulations. *Theor. Appl. Climatol.*, **50**, 117–131.
- Glynn, W. J., and R. J. Muirhead, 1978: Inference in canonical correlation analysis. *J. Multivariate Anal.*, **8**, 468–478.
- Hewitson, B. C., and R. G. Crane, 1992: Regional-scale climate prediction from the GISS GCM. *Paleogeogr. Paleoclimat. Paleocol.*, **97**, 249–267.
- Houghton, J. T., B. A. Callander, and S. K. Varney, Eds., 1992: *Climate Change 1992*. Cambridge University Press, 200 pp.
- Kass, E., T.-S. Li, and T. Schmith, 1996: Statistical hindcast of wind climatology in the North Atlantic and northwestern European region. *Climate Res.*, **7**, 97–110.
- Lal, M., L. Bengtsson, U. Cubasch, M. Esch, and U. Schlese, 1995: Synoptic scale disturbances of the Indian summer monsoon as simulated in a high resolution climate model. *Climate Res.*, **5**, 243–258.
- Livezey, R. E., 1995: The evaluation of forecasts. *Analysis of Climate Variability: Applications of Statistical Techniques*, H. von Storch and A. Navarra, Eds., Springer Verlag, 177–196.
- Lunkeit, F., M. Ponater, R. Sausen, M. Sogalla, U. Ulbrich, and M. Windelband, 1996: Cyclonic activity in a warmer climate. *Beitr. Phys. Atmos.*, **69**, 393–407.
- Manabe, S., R. J. Stouffer, M. J. Spelman, and K. Bryan, 1991: Transient responses of a coupled ocean–atmosphere model for gradual changes of atmospheric CO_2 . Part I: Annual mean response. *J. Climate*, **4**, 785–818.
- Mikolajewicz, U., B. Santer, and E. Maier-Reimer, 1990: Ocean response to greenhouse warming. *Nature*, **345**, 589–593.
- Schmidt, H., and H. von Storch, 1993: German bight storms analysed. *Nature*, **365**, 791.
- Trenberth, K. E., and D. A. Paolino, 1980: The Northern Hemisphere sea-level pressure data set: Trends, errors and discontinuities. *Mon. Wea. Rev.*, **108**, 855–872.
- von Storch, H., 1995a: Inconsistencies at the interface of climate impact studies and global climate research. *Meteor. Z. (NF)*, **4**, 72–80.
- , 1995b: Spatial patterns: EOFs and CCA. *Analysis of Climate Variability: Applications of Statistical Techniques*, H. von Storch and A. Navarra, Eds., Springer-Verlag, 227–258.
- , J. Guddal, K. A. Iden, T. Jónson, J. Perlwitz, M. Reistad, J. de Ronde, H. Schmidt, and E. Zorita, 1993a: Downscaling of climate change estimates to regional scales: Application to winter rainfall in the Iberian Peninsula. *J. Climate*, **6**, 1161–1171.
- , E. Zorita, and U. Cubasch, 1993b: Changing statistics of storms in the North Atlantic? MPI Rep. 116, 12 pp. [Available from Max-Planck-Institut für Meteorologie, Bundesstrasse 55, 20146 Hamburg, Germany.]
- WASA, 1995: The WASA project: Changing storm and wave climate in the northeast Atlantic and adjacent seas. *Proc. Fourth Int. Workshop on Wave Hindcasting and Forecasting*, Banff, AB, Canada, 31–44. [Available from GKSS, Institute of Hydrophysics, P.O. Box, 21502 Geesthacht, Germany.]